

THE CONSTRUCTION STATUS OF BEAM TRANSPORT LINE FROM XFEL-LINAC TO SPring-8 STORAGE RING

C. Mitsuda*, N. Azumi, K. Fukami, T. Fujita, H. Kimura, N. Kumagai, S. Matsui, M. Oishi, H. Ohkuma, Y. Okayasu, M. Shoji, K. Tsumaki and T. Watanabe

JASRI/SPring-8, Hyogo 679-5198, Japan

M. Hasegawa, Y. Maeda, T. Nakanishi, Y. Tsukamoto and M. Yamashita
SPring-8 Service Co. Ltd. (SES), Hyogo 678-1205, Japan

Abstract

The beam transport line from XFEL/Linac to SPring-8 storage ring is nearing to completion. The newly constructed line is 310 m, which is just a half of the whole path from the XFEL/Linac to the storage ring. Supposing that a bunch length and horizontal emittance at the exit of the XFEL/Linac are estimated about 30~100 fs and 0.04 nm-rad respectively, it is expected that the current beam emittance and bunch length in the SPring-8/Storage-ring (SR) is improved by a factor of about 100. The high brilliance and short pulsed synchrotron radiation light will be available in SR [1]. The conceptual design and construction status of the transport line will be presented with the emphasis on the detailed design and the fabrication of the magnets.

designed 13.4 m downstream of Sy ejection point. Finally, the beam orbit must be bended horizontally again by 6.8 degrees by switching magnet in order to join the existed beam transport (SSBT: booster Synchrotron to Storage ring Beam Transport line) line of 300 m from Sy to SR, then injected to the SR through SSBT. The beam orbit level from the floor is 1.2 m through whole lines. The design work of

THE BEAM TRANSPORT LINE

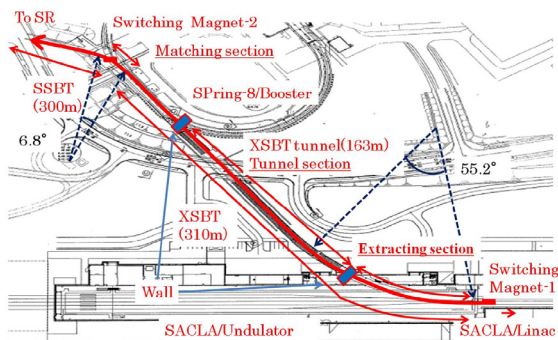


Figure 1: Overview of the beam transport line.

The construction of XFEL/SPring-8 (SACLA: SPring-8 Angstrom Compact Free Electron Laser) was completed in 2010 [2]. Figure 1 describes the overview of the beam transport line. The electron beam switched from SACLA is to be injected to the newly beam transport line (XSBT: XFEL-Linac to booster Synchrotron Beam Transport line), then connected to the ejection line of SPring-8/Booster synchrotron (Sy) at 310 m downstream of SACLA. So, the beam orbit must be bended horizontally by 55.2 degrees from SACLA orbit. Furthermore, the beam orbit must be bended down by 10.0 degrees and bended up again by 10.0 degrees in order to absorb the 9 m ground level difference between the SACLA and the Sy. The matching section is

* mitsuda@spring8.or.jp



Figure 2: The outside view of the XSBT tunnel.

the beam optics of XSBT was finished in 2008. The XSBT tunnel of 163 m to connect the SACLA with Sy was constructed as a part of beam transport line from 2008 to 2009. Figure 2 shows the outside view of the tunnel. The design and fabrication of the required magnet, vacuum, and beam diagnostic systems finished in 2009.

LATTICE DESIGN

As shown in previous section, the beam orbit is bended not only horizontally but also vertically. These conditions cause the emittance growth and bunch lengthening strongly by following effects: the dispersion and the contamination of coherent synchrotron radiation (CSR) [3] arise in the bending magnet sections. The Chasman-Green (CG, DBA: Double Bend Achromatic) lattice was adopted as an optics design for horizontal and vertical bending part to suppress the dispersion at least. After considering the lattice design, the dispersion was finally suppressed down to 0.57 m in a calculation. Additionally, the shape of the bending magnet was made in sector to reduce the dispersion caused by edge focus effect at the bending part. The lattice design for straight section of the beam line simply takes the FODO lattice. The SSBT will be used without modification for the near term. However, because the current SSBT is designed by the FODO lattice, it is predicted that the large emittance growth and large bunch lengthening will occur at the exist of the SSBT. Therefore, the

total considering of the lattice design involving the SSBT improvement is now being discussed. Figure 3 shows a

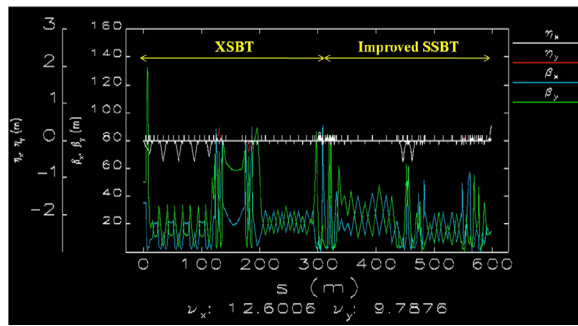


Figure 3: A twiss-parameter for the XSBT and improved SSBT.

preliminary result of the total optics design including both XSBT and SSBT. In the calculation, the CG lattice in improved SSBT is adopted by a same reason as XSBT. The improvement of the SSBT lattice can suppress the dispersion to the same level as XSBT. Based on the above result, assuming the energy spread of 0.1% in 8 GeV beam energy at SACLA, the beam conditions with the CSR effect for some beam operation options are summarized in table 1.

Table 1: Beam Parameter for Beam Operation Options

Beam parameter	SACLA /Linac	Up to XSBT	+cur. SSBT	+imp. SSBT
Emittance (nmrad)	0.04	0.2	0.4	0.4
Bunch length (ps)	0.1	0.2	20.0	0.5

DESIGN OF MAIN COMPONENTS

Vacuum System

Supposing that a beam emittance and an energy spread is 0.04 nmrad and 0.01~0.1 % respectively at the exit of the SACLA, the chamber size can be reduced correspondingly. However, the wake field caused in the chamber inner wall increases in inverse proportion to the distance between a beam and the wall. So, considering the wake field effect, the chamber inner diameter and inner height was decided to be 24.8 mm in quadrupole magnets and 24 mm in bending magnets. The chamber was made by SUS304 and connected by ICF70 flange each other. The designed vacuum pressure is 10^{-4} Pa.

Beam Diagnostic

Along the XSBT, 3 beam current monitors, 19 beam profile monitors and 5 strip-line type beam position monitors are installed. The beam position monitor was designed as it has about 100 μ m position resolution. The beam current is monitored by integrated current transformer (ICT). It is confirmed by our experiment [4] that the beam current measured by ICT does not depend on the bunch length

at least between 340 fs and 8.5 ps corresponding to a ultra short bunch length generated by the SACLA. About the beam profile monitor, both a OTR screen of thin Al plate and a Demarquest screen were mounted in a beam profile monitor system to capture the beam image for purposes.

Magnet System

The magnet types, the number of magnets and the magnetic field strength required from a lattice design are shown in Table 2. The flatness for a horizontal magnetic field

Table 2: Design Parameters for each Magnet Type

Type	# of magnets	Gap/Bore rad.	Field /Gradient	Magnet length
BH(Hor.)	9	30.0	1.2 T	2.252 m
BV(Ver.)	4	30.0	1.2 T	1.941 m
QA	8	29.0	68.81 T/m	200 mm
QB	30	29.0	47.40 T/m	200 mm
QC	16	29.0	13.35 T/m	200 mm
StH/StV	10/10	40.0	0.76 T	200 mm

distribution in ± 5 mm region was designed 1×10^{-4} for bending magnets and 1×10^{-3} for quadrupole magnet. In a magnet design, it is important to decrease the magnet yoke volume keeping the flatness and field strength.

For downsizing the magnet yoke volume, the return-yoke and pole were optimized to be thinner as much as possible. To increase structural strength with thinner yoke, the window frame shape as a cross-section structure was adopted for the bending magnets. This structure gives a good magnetic field symmetry also. For downsizing the quadrupole magnet, the magnet was design by same design concept as bending magnet. The downsizing of yoke volume without any optimizations makes a field strength weak. To prevent the field strength from decreasing, the pole shape and shim shape was optimized with MAFIA simulation code, including the pole and return yoke width optimization. The table 3 shows the design values. The final cross-sectional size of B and Q type magnets could be shrunk to 324(H) \times 470(W) mm and 330(H) \times 330(W) mm respectively. The number of power supply for bend-

Table 3: Magnet Design Values

Type	Flux (AT/pole)	Hollow conductor	Field strength and Flatness
B	300 \times 54	11.0 \square \times Φ 6	1.2(T)/3.0 $\times 10^{-5}$
QA	220 \times 32	7.5 \square \times Φ 4.5	68.80(T/m)/7.4 $\times 10^{-4}$
QB	220 \times 22	7.5 \square \times Φ 4.5	54.17(T/m)/1.0 $\times 10^{-3}$
QC	25 \times 50	3 \times 8	14.78(T/m)/8.7 $\times 10^{-4}$

ing magnets, quadrupole magnets and steering magnets are prepared 6, 20 and 20. Their long-term fluctuation in the output current is less than $\pm 1 \times 10^{-4}$.

Since the XSBT is separated with three sections by the 4.4 m concrete wall, the alignment base points were

Table 5: Measurement Results of Field Strength and Size Variation

Type	Ave. field strength (to cal./to spec.)	BL/GL to spec. (%)	Flatness	Field strength var. (%)	Magnet length dev. ($\mu\text{m}(\%)$)	Gap/Bore dev. ($\mu\text{m}(\%)$)
BH/BV	1.23 T (-2.4%/+2.5%)	+4.2/+4.1	$<1.0/1.6 \times 10^{-4}$	0.09	$<100(0.004)$	0.018(0.6)
QA	64.08 T/m (-6.9%/-6.9%)	+0.1	3.2×10^{-3}	0.21	0.006(0.003)	0.036(0.12)
QB	51.43 T/m (-5.3%/+2.3%)	+10.5	1.0×10^{-3}	0.12	0.007(0.004)	0.017(0.06)
QC	14.90 T/m (+1.0%/+10.4%)	+21.7	1.0×10^{-3}	0.13	0.008(0.004)	0.019(0.07)

copied from SACLA/Undulator building and SPring-8/Sy to XSBT tunnel both on the upper and lower level of the slope. The horizontal position error was absorbed by bending angle and displacement of the horizontal bending magnet in upslope of XSBT tunnel. The magnets were aligned by a laser tracker (T3, API Co. Ltd.) of ± 5 ppm and level of 0.05 mrad. The alignment results were shown table 4. The alignment tolerance in the table were decided based on the simulation results of beam oscillation caused by the magnet position error. This alignment tolerance has a possibility to cause the 6 mm beam oscillation.

Table 4: Alignment Tolerances and Results

Direction	Allowed accuracy	Ave. Results B/Q
Horizontal Δx	0.2 mm	0.03/0.05 mm
Vertical Δy	0.2 mm	0.03/0.03 mm
Longitudinal Δs	0.5 mm	0.1/0.04 mm
Rotation $\Delta\theta_{x,y,s}$	0.2 mrad	0.06/0.06 mrad

MAGNET FABRICATION

All of the magnet types were made by massive iron yoke. For bending magnets, the return yoke was built up by mill rolling plate and the poles were attached to mill role plate by long bolts after being cut from massive iron with numerical control machining (NC) by a precision of $5 \mu\text{m}$. For quadrupole magnets, after the pole was cut from massive iron by NC for each four-quadrant, they also were built up by long bolts. The magnets of all type can be separated in median-plane to install a vacuum chamber. The precision of building up of the half-upper side magnet and half lower side magnet was ensured by pinning structure in the contacting surface. The target plate which was put on the magnet was designed to be put the laser tracker target holder for alignment and made by a rotation error of 0.02 mrad. The measurement results of field strength for a horizontal distribution in the magnet center and size variation for the fabricated magnet is shown in table 5. The field strength was measured by a hall-element probe. In the case of QA and QB type magnet, the measured fields were smaller than calculated one. This differences are came from the difference between B-H curve used in calculation and the measured one of actual SUY-0 iron yoke. The field saturation of actual B-H curve started from lower field region than the one used in simulation. The integrated field strength of all of the magnets met the required specification conclu-

sively. The field strength variation was suppressed sufficiently small for horizontal distribution. This results were came from the good fabrication precision of massive iron yoke.

For bending magnets, the trouble of mismatching between upper side yoke and lower side yoke happened. Since the BL variation of up to 4×10^{-3} was confirmed by precious integrated field measurement, the negative influence to the optics was reduced by considering the combination between power supply and magnet connected to it. The field flatness met required specification and matched the calculation except for QA type whose flatness was degraded compared with calculation due to B-H curve difference described above. It was concluded that the magnets were fabricated with the field strength and the field accuracy needed in beam operation as a whole.

STATUS AND NEAR FUTURE PLAN

In 2010, the construction of the beam line and the installation of main components almost finished. Figure 4 shows the accomplished extracting section and tunnel section without vacuum chamber, in which the most right hand side beam line is XSBT directing to the XSBT tunnel. We will start tuning and to inject the electron beam from SACLA to SPring-8/Sy's dump line in the near future.



Figure 4: The completed extraction section and the slope of tunnel section after main component installations.

REFERENCES

- [1] T. Masaki, et. al, THPC028, in these proceedings.
- [2] H. Tanaka, et. al, MOYCA01, in these proceedings.
- [3] K. Fukami, et. al, Proc. Annual meeting of Particle accelerator Society of Japan, Himeji, Japan, 2009, p1218
- [4] T. Watanabe, et. al, Proc. Annual meeting of Particle accelerator Society of Japan, Toukai, Japan, 2008, p310